CONTACT ANGLE AND SURFACE TENSION FROM SESSILE AND PENDANT DROP PERTURBATION SOLUTIONS [1]

J. Fuentes[2] and A. L. López de Ramos[2,3]

---

[1] Paper presented at the Thirteenth Symposium on Thermophysical Properties, June 22-27, 1997, Boulder, Colorado, USA.

[2] Grupo FTUSB. Departamento de Termodinámica y Fenómenos de Transferencia. Universidad Simón Bolívar. Apartado Postal 89.000. Caracas 1080-A. Venezuela.

[3] Author to whom all correspondence should be addressed.

ABSTRACT

The Laplace-Young equation can be solved approximately using perturbation methods [1, 2, 3 and 4]. In all cases, the perturbation results were compared with numerical solutions of Hartland and Hartley [5] but they were never compared with experimental profiles. In this work, the O'Brien's Second-Order Solutions [3] were improved by algebraic simplifications and the singularity presented near $\phi=0$ was eliminated. The second-order relationship were very simple and it was not necessary to use the limit of the functions to evaluate it at $\phi = 0$. Also a new method was developed to calculate the surface tension using O'Brien solutions. All the ultimate methods were used to compute surface tension and contact angles values from experimental drop profiles from different fluids. A friendly Windows' application was developed to calculate surface tension using these methods. The results have a good agreement between them, the differences in all the cases were less than 10%.

KEYWORD: contact angle, experimental method, hydrocarbon-air system, Laplace-Young equation, perturbation method, surface tension.

INTRODUCTION

The shape of liquid drops (sessile and pendant) can be described by the Laplace-Young equation. This equation is just a balance between gravity, hydrostatic pressure, and surface tension effects. When drops are axisymmetric, the Laplace-Young equation can be written as:

$$\sigma\left(\frac{1}{R_1}+\frac{1}{R_2}\right)=\pm\rho g y+\frac{2}{R_0}$$

(1)

where σ is the surface tension, R_1 and R_2 are the principal radii of curvature, ρ is the liquid density, g is the gravitational acceleration and R_0 is the radius of curvature at y=0 (Fig. 1). The term $\left(\frac{1}{R_1}+\frac{1}{R_2}\right)$ is the mean curvature of the drop, this curvature is a function of the y position and can be expressed using differential geometry as[6]:

$$\left(\frac{1}{R_1}+\frac{1}{R_2}\right)=\frac{d^2y/dx^2}{\left[1+\left(dy/dx\right)^2\right]^{3/2}}+\frac{dy/dx}{x\left[1+\left(dy/dx\right)^2\right]^{1/2}}$$

(2)

With the definition of curvature given in Eq. (2), Eq. (1) can be reduced to an ordinary, nonlinear second order differential equation and can be numerically integrated. The Laplace-Young equation written in a parametric form —x=x(s) and y=y(s), where s is the arc length measured from the drop apex— can be solved approximately using perturbation methods [1,2,3,4].

The objective of this work was to apply the perturbation solutions [2,3,4] to experimental pendant and sessile drops profiles in order to compute surface tension and contact angle for different liquid-gas-solid systems.

MATHEMATICAL MODEL

The Laplace-Young equation written in a parametric form (*i. e.* in terms of the arc length, s) is:

$$\sigma\left(\frac{d\phi}{ds}+\frac{\sin\phi}{x}\right)=\pm\rho gy+\frac{2}{R_0}$$

(3.a)

$$\frac{dx}{ds}=\cos\phi$$

(3.b)

$$\frac{dy}{ds}=\sin\phi$$

(3.c)

where ϕ is the inclination at any point (x, y) and s is the arc length measured from the apex (Fig. 1). The advantage of the system of first-order equations (Eq. 3) over the second-order equation (Eqs.1 and 2) is that there is no longer problems with the first order derivatives when the profile of the drop becomes vertical (at $\phi=\pi/2$).

As the arc length is of no particular interest, O'Brien and van den Brule [2] proceed to eliminate it from the system of equation (Eq. 3). They obtained an expression for $d\phi/ds$ and, then dividing this in turn by Eqs. (3.b) and (3.c), they found:

$$\frac{dx}{d\phi}=\frac{\sigma x\cos(\phi)}{\pm\rho gxy+\frac{2}{R_0}x-\sigma\sin(\phi)} \qquad \frac{dx}{d\phi}=\frac{\sigma x\sin(\phi)}{\pm\rho gxy+\frac{2}{R_0}x-\sigma\sin(\phi)}$$

(4)

The boundary conditions were:

$$\phi=0\rightarrow\begin{cases}x=0\\y=0\end{cases}$$
$$\phi=\pi/2\rightarrow x=L \text{ or } D_E/2$$

(5)

where 2L (or D_E) is the maximum diameter of the drop.

Defining $x = RX$; $y = RY$ and $2/R_0 = P/R$, $\varepsilon = R^2$, where R is the dimensionless radius ($R = L(g\rho/\sigma)^{1/2}$), the system of equation (4) reduces to:

$$\frac{dX}{d\phi} = \frac{X\cos(\phi)}{\pm\varepsilon XY + XP - \sin(\phi)} \qquad \frac{dY}{d\phi} = \frac{X\sin(\phi)}{\pm\varepsilon XY + XP - \sin(\phi)}$$

(6)

The scaled boundary conditions are:

$$\phi = 0 \rightarrow \begin{cases} X = 0 \\ Y = 0 \end{cases}$$
$$\phi = \pi/2 \rightarrow X = 1$$

(7)

The solutions of equations are seek in the following form [2,3,4]:

$$\begin{cases} X = X_0 \mp \varepsilon \cdot X_1 + \varepsilon^2 \cdot X_2 \\ Y = Y_0 \mp \varepsilon \cdot Y_1 + \varepsilon^2 \cdot Y_2 \\ P = P_0 \mp \varepsilon \cdot P_1 + \varepsilon^2 \cdot P_2 \end{cases}$$

(8)

Zero-Order Solutions [2,3,4]:

$$\begin{cases} X_0 = \sin(\phi) \\ Y_0 = 1 - \cos(\phi) \\ P_0 = 2 \end{cases}$$

(9)

First-Order Solutions [2,3]:

$$\begin{cases} X_1 = -1/3 \cdot \cos^2(\phi) \cdot \tan(\phi/2) \\ Y_1 = -1/3 \cdot \cos(\phi) + 1/3 \cdot \cos^2(\phi) - 2/3 \cdot \ln[\cos(\phi/2)] \\ P_1 = 1/3 \end{cases}$$

(10)

Second-Order Solutions

With respect to the Second-Order Solution, the O'Brien's solutions was very troublesome and presented a singularity at $\phi = 0$ and $\phi = \pi$. The problem in $\phi = \pi$ is because an incorrect scaling near this region was used, and it was found that a boundary layer occurs in this part of the drop [3]. In our work, the O'Brien's Second-Order Solutions was improved by algebraic simplifications. Additionally, the singularity presented near $\phi = 0$ was eliminated. The second-order solution becomes very simple and it is not necessary to use the limit of the functions to evaluated it at $\phi = 0$. The equations obtained are:

$$\begin{cases} x_2 = -1/6 \cdot \sin(\phi) \cdot \ln[\cos(\phi)+1] + \\ 1/18 \cdot \sin(\phi) \cdot \cos(\phi) \cdot \left[4 \cdot \cos(\phi)^3 + 2 \cdot \cos(\phi)^2 - \cos(\phi) + 3\right] \Big/ \left[\cos(\phi)+1\right]^2 \\ y_2 = 1/6 \cdot \ln(2) + 1/6 \cdot [\cos(\phi) - 2] \cdot \ln[\cos(\phi)+1] - \\ 1/18 \cdot \cos(\phi) \cdot [\cos(\phi) - 1] \cdot \left[4 \cdot \cos(\phi)^2 + 2 \cdot \cos(\phi) - 5\right] \Big/ [\cos(\phi)+1] \\ p_2 = 1/3 \cdot \ln(2) - 1/6 \end{cases}$$

(11)

The perturbation solution can be used to computer the contact angle and surface tension from the shape of small sessile and pendant drops. For contact angles O'Brien and van der Brule [2] recommended three different ways to compute contact angles. All three methods were followed in this work using and experimental sessile drop profile to calculate the contact angle values.

EXPERIMENTAL EQUIPMENT

In order to create pendant or sessile drops, a high pressure cell was designed to work up to 5,000 psia (34.5 MPa) and 212 °F (373.15 K). The cell consists of a metal body (stainless steel) and has two Pyrex windows. The windows are sealed to the cell body through grafoil (1/16 inch of thickness). The liquid phase can be introduced into the cell from the top or from the bottom in order to create pendant or sessile drops. A surgical needle inserted at the top of the cell is used to form pendant drops. A small hole on the bottom surface allows the formation of sessile drops, but also a needle can be inserted

from the hole, in case that emergent or captive drops are desired. There is a gas entrance in one of the sides and a thermocouple well in the other. Four channels spanning the width of the cell are used to circulate water, keeping the temperature constant inside the cell. The circulating water temperature is controlled using a constant temperature bath. Figure 2 is a schematic view of the complete experimental setup for the high pressure cell.

The cell is illuminated from the back using a fiber optic lamp. A diffuser is placed between the lamp and the rear window. A video camera (CCD-72 from DAGE-MTI Incorporated) is located at the front window. Two lenses can be attached to the video camera through a C connector. One of the lenses is the Nikkon 55 mm micro with a PK-13 extension ring and the other lens is the D. O. Industries Zoom 6000 Microscopic. The pendant drop image can be captured easily and it can be sent to the video recording system (Panasonic AG-7300) or to the computer (using the Targa® videographic system connected to Intel®80586-100 Mhz CPU with VGA card and monitor). The image visualization equipment is also furnished with a Sony PVM2530 RGB monitor. The cell and the optical components are placed on an Oriel optical tubular bench with vibration isolation legs. Figures 3 and 4 show pendant and a sessile drops before and after the computer image analysis. From the drop image outlines the xy profiles are obtained using a program in Visual-Basic. A friendly Windows' application was developed to calculate surface tension and contact angle using different methods. Figure 5 shows an esquematic description of the main structure of the program.

Several pendant drop experiments were made at low pressure. The liquid used decane (99+%, Aldrich), decy alcohol (99+%, Aldrich), hexadecane (99%, Aldrich), toluene (99%, Aldrich), heptane (99%, Aldrich) and 2,2,4-trimethylpentane (99+%, Aldrich). The gas phase used was air at 25°C and 1 atm. For sessile drop the system mercury-air-glass was used.

RESULTS AND DISCUSSION

The perturbation solution is a series of functions that it must converge to the correct value when the number of terms goes to infinite. In this work, Eq. (3) was cut in the third term. The error in the series can be calculated through the difference between the numerical solution (Runge-Kutta 4th order) of Eq. (6) and the perturbation solution (Eq. (8)). This error is a function of the maximum drop radio $(D_E/2)$ and the value of the point inclination (f). On Table 1, there are presented the maximum drop radius that is possible to allow if a maximum percent error in the series is impost (1 to 10%). The perturbation solution was developed for drops with relatively small radii.

A theoretical water profile for a pendant drop was generated by numerical integration of Laplace-Young equation. Both, the theoretical profile and the second-order perturbation solution are presented in the Fig. 6. In this case, the dimensionless maximum drop radio (R) is 0.618729035. From Table 1.a, with an error less than 5%, the perturbation solution is a good approximation between the range of [0, ½ π]. This agree with the results presented at the Fig. 6. A comparison between the perturbation solution and an experimental profile for decane was done (Fig. 7). From these results, it can be concluded that the accuracy of the perturbation equations depends on the following parameters: the maximum diameter of the drop and the total points of the drop profile taken into account (ϕ value).

The new method developed to calculate the surface tension using O'Brien solutions was based on the searching of a correction factor. This factor was calculated by comparison of the D_E value from the perturbation and Runge-Kutta solutions. On Table 2 are reported the surface tension values calculated by the O'Brien's perturbation solutions and those values obtained using the correction factor found in this work. For all the cases, the corrected values are higher than those predicted by the O'Brien's solutions.

When the complete set of O'Brien solutions was put together in order to compute surface tension values from the complete profiles of pendant drops, the results were extremely poor, as it can be seen in Fig. 8 (ε=0.8). To obtain drops with small values of ε is not always experimentally possible. This correction factor allows to apply perturbation solution to medium sized drops with an acceptable accuracy.

Table 2 summarizes all the results for the systems studied. Typical experimental pendant drop profiles contain more than 400 data points. In general, there is a good agreement between the surface tension obtained for the spline methods and the Hansen and Rødsrud's technique [7], and those collected by Jasper [8].

Table 3 shows all contact angle values calculated by perturbation solution using the three methods suggested by O'Brien and van der Brule [2]. Notice that the results, in general, have an acceptable repeatability.

CONCLUSION

The perturbation solutions for a sessile drop can be used to calculated the contact angle knowing the maximum radius and drop height. The solution for the bottom of a pendant drop can be used to compute surface tension values.

LIST OF SYMBOLS

D_E:	Maximum diameter of the drop.
g:	Gravitational acceleration.
L:	Maximum radius of the drop.
P:	Variable define on Eq. (6).
R:	Dimensionless radius.
R_0:	Apex radius of curvature.
R_1 and R_2:	Principal radii of curvature.
s:	Arc length measured from the drop apex.

x: Independent variable.

X: Dimensionless variable defined on Eq. (6).

y: Axial coordinate.

Y: Dimensionless variable defined on Eq. (6).

ε: Variable defined on Eq. (6).

ϕ: Inclination at any point.

ρ: Liquid density.

σ: Surface tension.

ACKNOWLEDGMENTS

The authors want to thank the *Decanato de Investigaciones y Desarrollo* of the *Universidad Simón Bolívar* and *CONICIT* (Project N° S1-95-000476) for their financial support.

REFERENCES

[1] A. K. Chester, J. Fluid. Mech., **81**,4 (1977) 609-624.

[2] B. G. M. O'Brien and B. H.A. A. van den Brule, J. Chem. Soc. Faraday Trans., **87**, 10 (1991) 1579-1583.

[3] S. B. G. O'Brien, J. Fluid. Mech., **233** (1991) 519-537.

[4] S. B. G. M. O'Brien, Quarterly of App. Math., **LII**, 1 (1994) 43-48.

[5] S. Hartland and R. W. Hartley, Axisymmetric Fluid Interfaces. Elsevier. 1976.

[6] L. E. Scriven, Surface Geometry for Capillarity, ChEn 8104 Course Handout, University of Minnesota, 1981.

[7] F. K. Hansen and G. Rødsrud, Journal of Colloid and Interface Science, **141**, 1 (1990) 1-9.

[8] Jasper, J. "The Surface Tension of Pure Liquid Compounds", *J. Phys. Chem. Ref. Data*, **1**, 841-1009, (1971).

Table 1.a Dimensionless Maximum Drop Radio [Pendant Drop]

Interval	1 %	5 %	10 %
0 - ¼ π [rad]	≤ 0.721307433	≤ 1.05889275	≤ 1.237080174
0 - ½ π [rad]	≤ 0.553145002	≤ 0.854197032	≤ 1.047901276
0 - ¾ π [rad]	≤ 0.291594222	≤ 0.425484714	≤ 0.494986404

Table 1.b Dimensionless Maximum Drop Radio [Sessile Drop]

Interval	1 %	5 %	10 %
0 - ¼ π [rad]	≤ 0.731951052	≤ 1.093456621	≤ 1.293209846
0 - ½ π [rad]	≤ 0.534571904	≤ 0.790183473	≤ 0.935881764
0 - ¾ π [rad]	≤ 0.298915124	≤ 0.449255187	≤ 0.533576983

Table 2. Surface Tension Values [dynes/cm] from Pendant Drop.

Liquid	Jasper	Hansen & Rødsrud	López *et. al.*	O´Brien & van der Brule	This work
Decyl Alcohol	28.6	25.3	25.7	23.1	25.6
Toluene	28.1	25.6	25.5	23.1	25.7
Hexadecane	27.1	23.7	24.3	23.4	25.8
Heptane	19.7	19.4	19.6	18.5	20.5
2,2,4-Trimethyl Pentane	18.4	18.1	18.1	17.5	19.5
Decane	23.5	22.3	22.2	20.7	22.8

Table 3: Contact Angle Values [dynes/cm] from Sessile Drop.

Substance	Contact angle perturbation ±1°	Contact Angle goniometer ±1°
Mercury-air-glass	132	132°
NaOH(0.01M)-air-aspirin	53	52
NaOH(0.04M)-air-aspirin	56	57
NaOH(0.06M)-air-aspirin	60	61
NaOH(0.07M)-air-aspirin	61	61
NaOH(0.10M)-air-aspirin	72	73
NaOH(0.01M)-air-Benzoic acid	59	60
NaOH(0.04M)-air-Benzoic acid	61	61
NaOH(0.06M)-air-Benzoic acid	65	66
NaOH(0.07M)-air-Benzoic acid	67	69
NaOH(0.10M)-air-Benzoic acid	73	71

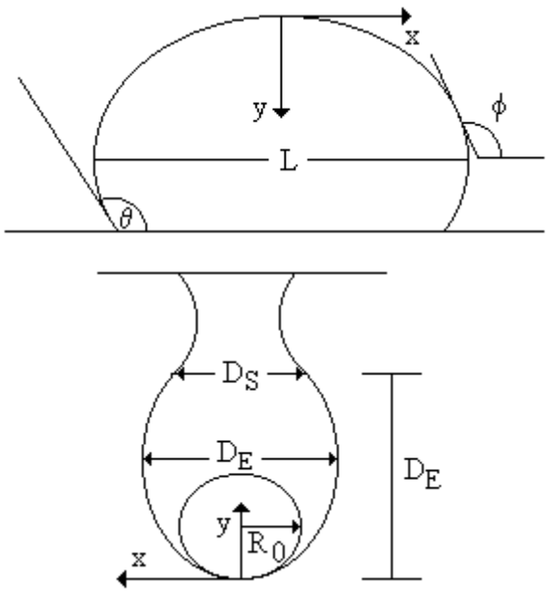

Fig. 1 Pendant (a) and Sessile (b) drop showing the geometrical variables.

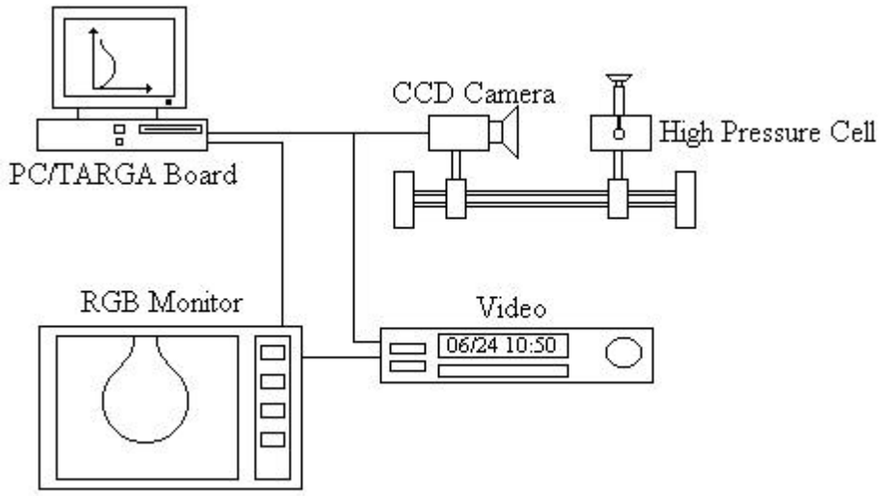

Fig. 2 Experimental set-up of the equipment used to obtain TGA images from sessile and pendant drops.

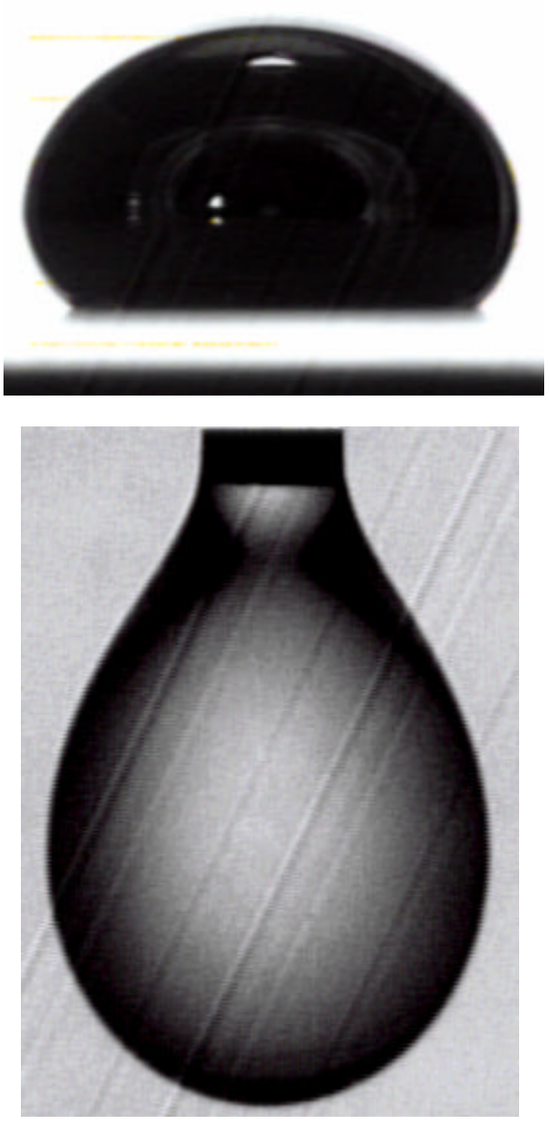

Fig. 3 Original image (TARGA format) for sessile and pendant drops.

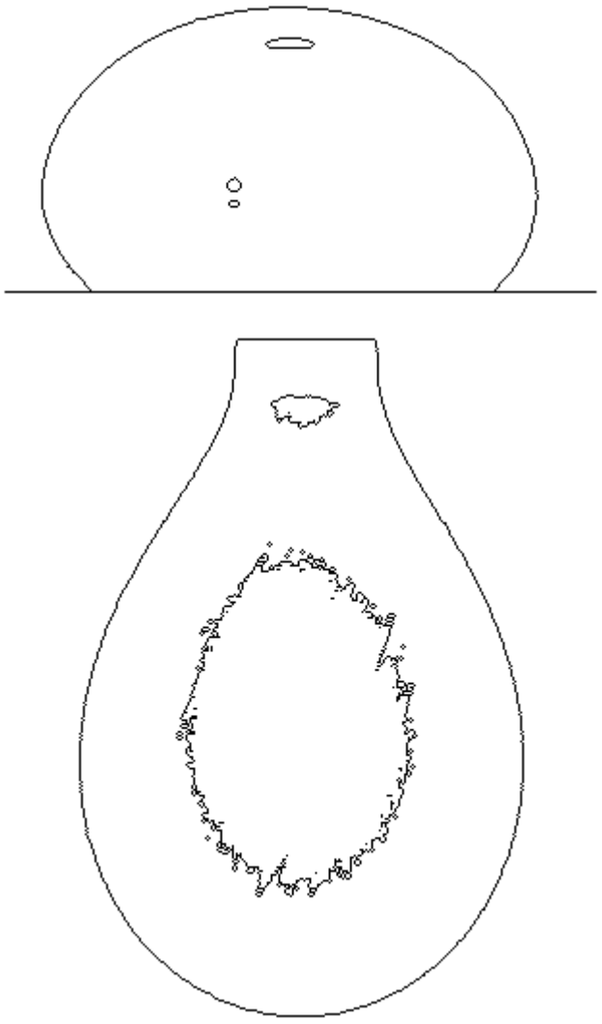

Fig. 4. Sessile and Pendant drop images after the computer image analysis.

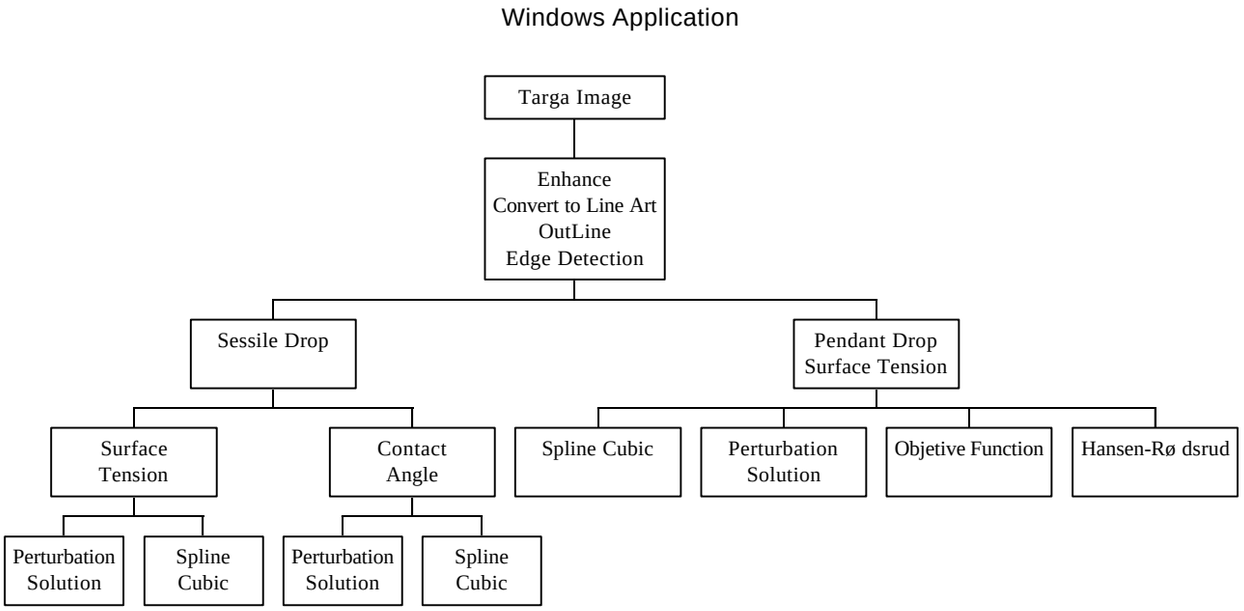

Fig. 5. Esquematic description of the Windows' application.

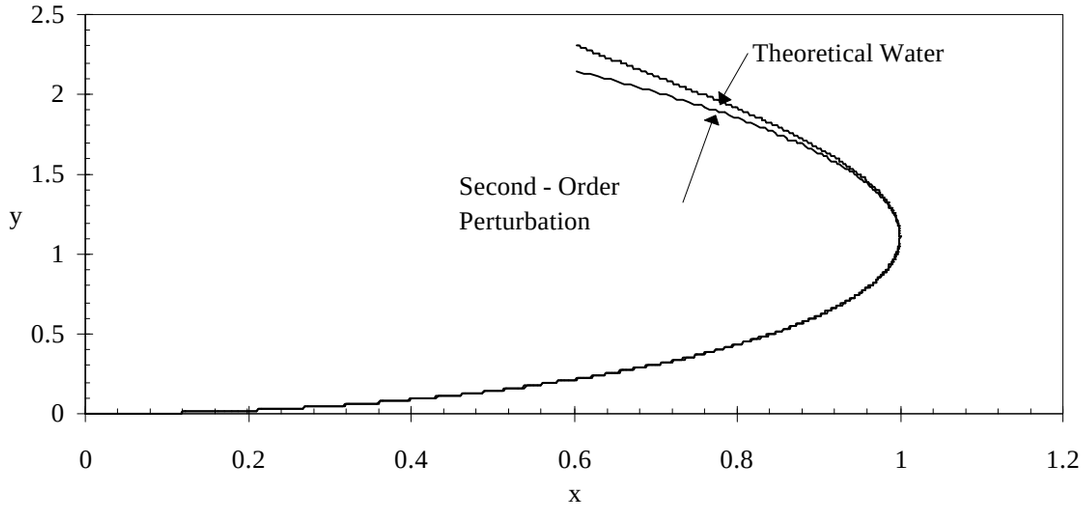

Fig. 6. Theoretical and the second-order perturbation water profile.

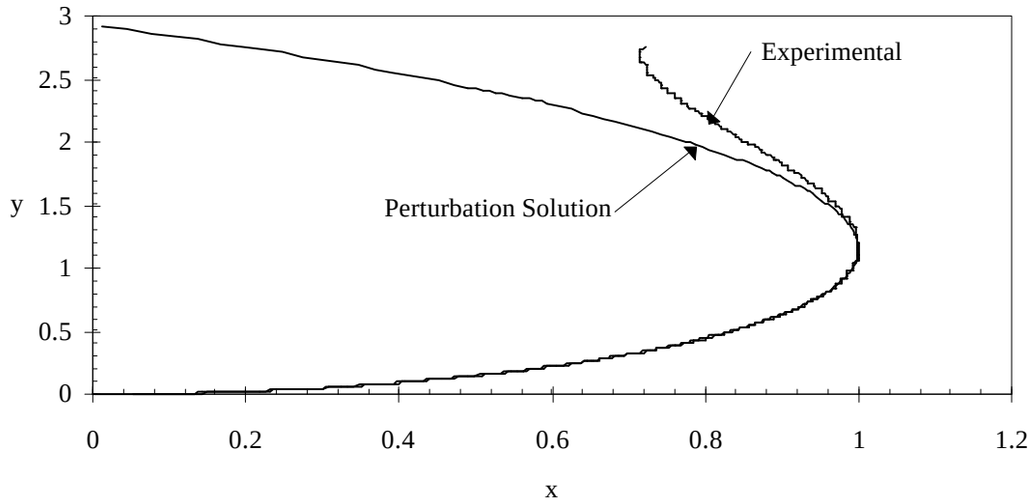

Fig. 7. Experimental and the second-order perturbation decane profile.

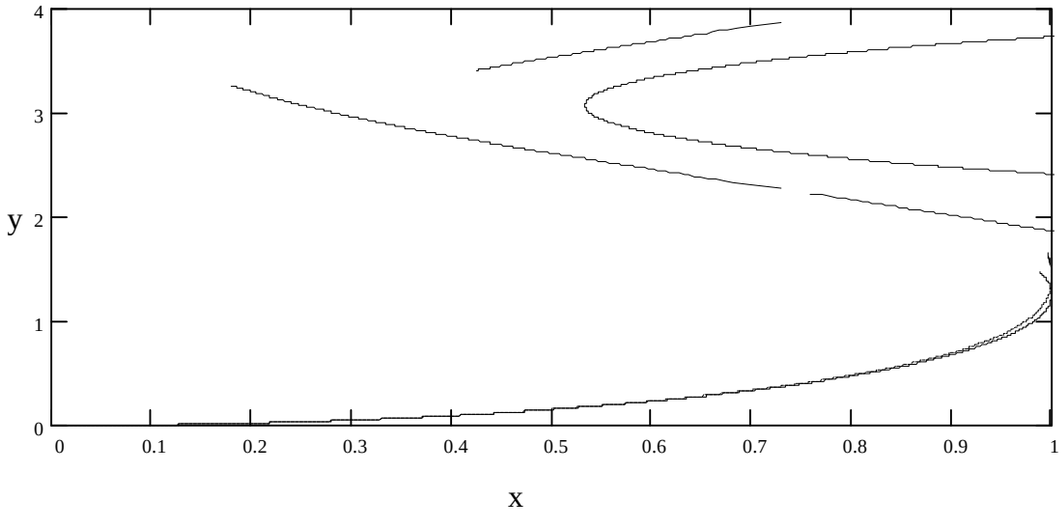

Fig. 8. Complete set of O’Brien solution of pendant drop.